

Evaluating the Gaseous Chlorine-containing Byproducts from the Use of an HOCl-derived  
Disinfectant

Tianyi Xu

A thesis  
submitted in partial fulfillment of the  
requirements for the degree of

Master of Science

University of Washington  
2025

Committee:  
Joel Thornton  
Robert Synovec

Program Authorized to Offer Degree:  
Chemistry

©Copyright 2025

Tianyi Xu

University of Washington

**Abstract**

Evaluating the Gaseous Chlorine-contained Byproducts from the HOCl Disinfectant

Tianyi Xu

Chair of the Supervisory Committee:

Joel Thornton

Department of Atmospheric Science and Climate Science

This study investigates the gas-phase chlorine-containing byproducts generated from HOCl solutions under controlled conditions using Time-of-Flight Chemical Ionization Mass Spectrometry (TOF-CIMS). We analyzed how delivery flow rate, ambient humidity, and nebulization time influence the speciation and concentration of volatile  $\text{Cl}_2$ , HOCl, and  $\text{NCl}_3$  within a sealed Teflon environment using relatively clean, compressed house air as the medium. Our results show that increasing the delivery flow rate enhances the detection of volatile HOCl while suppressing  $\text{Cl}_2$  levels, suggesting that in the absence of strong delivery flow,  $\text{Cl}_2$  dominates the headspace composition. Humidification of the carrier air substantially increased  $\text{Cl}_2$  formation while accelerating the decomposition of HOCl. The use of clean house air led to minimal  $\text{NCl}_3$  levels under the majority of conditions. These findings demonstrate the capability of TOF-CIMS to identify and quantify gaseous chlorinated byproducts with high time resolution and highlight the potential hazards of using HOCl-based disinfectants in poorly ventilated environments. Future experiments will focus on localized HOCl application to authentic

laboratory / office furniture near the IMR inlet and refined stepwise dosing protocols to support calibration curve development and health risk estimation.

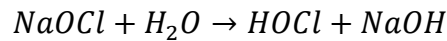
# Acknowledgements

I'm extremely grateful to my professor and chair of my committee, Professor Joel Thornton, for his valuable patience, mental support, and all-round guidance. I also would like to express my deepest gratitude to my defense committee, Professor Robert Synovec, for his kindness and expertise. Additionally, I am also thankful to my mentor and group member, Dr. Phil Rund, for his knowledge and feedbacks. And I am sending my appreciation to our postdoc, Christopher Kenseth, for his technical support on the instrument and equipment. Thanks should also go to my friend, Tingxuan Liu, who impacted and inspired me. Lastly, I'd like to mention my family. Their firm financial support and mental accompany are my strongest backup on the journey of research.

## Introduction

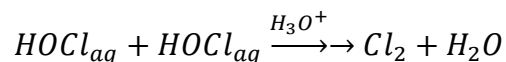
### 1. Background

Hypochlorite compounds have become the most commonly used disinfectants on the market today due to their rapid efficacy and low cost. They are typically available in liquid form as sodium hypochlorite (NaOCl) and in solid form as calcium hypochlorite (Ca(OCl)<sub>2</sub>). Upon dissolution in water, hypochlorite releases hypochlorous acid (HOCl),

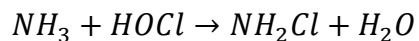


which serves as the primary antimicrobial active ingredient responsible for disinfection. (William and David, 2023) HOCl is widely recognized for its antimicrobial efficacy, primarily attributed to its ability to denature proteins and induce lipid peroxidation, thereby altering the properties of biological molecules. Therefore, hypochlorite-based disinfectants are commonly applied in indoor environments, such as households, through methods including wiping, mopping, and even nebulization into mist, in order to achieve effective microbial disinfection.

However, due to its inherent instability (Winterbourn, 2002), HOCl rapidly reacts with environmental constituents upon application, potentially leading to the formation of unwanted disinfection byproducts. These byproducts include, but are not limited to, molecular chlorine and chloramines (Wong et al., 2017). Under acidic conditions or at temperatures exceeding 25 °C, HOCl can convert into molecular chlorine (Cl<sub>2</sub>) through a multi-step mechanism.



Additionally, HOCl is susceptible to photodegradation and readily decomposes upon exposure to ultraviolet (UV) light (Masayuki et al., 2017). HOCl also reacts with ammonia (NH<sub>3</sub>) to form chloramines.



When present in significant concentrations, these compounds can pose serious risks to respiratory health (Stubbs et al., 2023), including conditions such as asthma and rhinitis, or even death.

Given these potential health hazards associated with chlorinated disinfection products and the byproducts of their use, it is imperative to monitor, quantify, and evaluate human exposure to these chlorinated byproducts following the use of chlorine-based disinfectants or bleaching agents.

Chlorine gas emissions from chlorinated cleaning agents and disinfectants have long been a concern for researchers. Regarding surface cleaning, literature indicates that using a personal passive air sampler (PPAS), with polydimethylsiloxane (PDMS) as the permeable medium, o-dianisidine as the redox dye, and calibration for Cl<sub>2</sub> performed using a Proton Transfer Reaction/Selective Reagent Ionization-Mass Spectrometer (PTR/SRI-MS), it was possible to quantify that after using disinfectants for indoor cleaning for more than 40 minutes in a 3 m<sup>3</sup> bathroom, chlorine exposure concentrations range between 100 and 400 ppbv (Ha et al., 2020). And from another research, the researchers used a direct-read instrument (Dräger Pac 7000 passive diffusion sampler) to measure the gaseous Cl<sub>2</sub> concentration in another bathroom with an approximate volume of 8 cubic meters following the use of cleaning products. Their results

claimed that in a 20-minute cleaning session, chlorine levels ranged between 0.09 ppm and 1.24 ppm, with a mean concentration of 0.55 ppm (Lindberg et al., 2021).

The decomposition byproducts of these disinfectants also vary depending on the indoor ventilation conditions. In unventilated indoor environments, after spraying disinfectants, chlorine concentrations gradually increase to a steady level unless further human intervention occurs (Stubbs et al., 2023). Conversely, in ventilated spaces, chlorine concentrations rise rapidly after spraying disinfectants and then quickly return to baseline levels (Mattila et al., 2020). Different measurement methods yielded varying concentrations, and different ventilation conditions resulted in distinct concentration profiles. This variability highlights the challenges inherent in accurately quantifying chlorine-containing byproducts following the use of chlorine-based disinfectants. The objectives of this study are threefold: (1) to evaluate the capability of the TOF-CIMS instrument, along with a custom-built Ion–Molecule Reactor (IMR), to detect and quantify trace level  $\text{Cl}_2$ , HOCl, and various chloramines; (2) to simulate different usage scenarios and qualitatively and quantitatively assess the formation of  $\text{Cl}_2$ , HOCl, and chloramine species following the application of HOCl disinfectants; and (3) to estimate the safe usage duration of HOCl disinfectants in enclosed environments, defined as the time required for the  $\text{Cl}_2$  level to reach 1 ppm as OSHA regulation indicated.

## **2. Method Outline**

In this study, we utilized a HOCl-based disinfectant produced by Briotech, which is formulated using low-percentage hypochlorous acid and electrolyzed water. With this HOCl solution, we simulate the application of two different HOCl disinfectant formulations under conditions that reflect real-world usage. By systematically varying environmental parameters such as humidity

and utilizing high-resolution time-of-flight chemical ionization mass spectrometry (TOF-CIMS), we investigate the formation and evolution of gas-phase chlorine chemistry based on HOCl usage.

The first approach employed in this study is referred to as the headspace experiment. By utilizing HOCl-based cleaning solutions, volatile compounds can accumulate in the headspace—the air volume above the liquid. Upon opening the container for use, or after utilizing the disinfectant, these gases may pose a potential exposure risk. Therefore, our initial objective was to analyze the chemical composition of the headspace volatile gases associated with the HOCl solution.

For the *headspace experiment*, we evaluated three different gas delivery methods to investigate the evolution of volatile species from the HOCl solution.

**Open-Air Diffusion Sampling (Static):** The opening of the native container was placed directly beneath the instrument inlet. Headspace gases were drawn into the instrument via its own vacuum system during operation, allowing for direct sampling without additional gas flow.

**Sealed Inert Flow Sampling (Dynamic Headspace, Passive Outgassing):** A defined volume of HOCl solution was placed into a Teflon-sealed gas delivery setup. High-purity nitrogen (N<sub>2</sub>) was used to gently carry the naturally outgassed headspace volatiles into the instrument without disturbing the solution.

**Bubbling Delivery (Dynamic Headspace, Active Stripping):** Building upon the sealed Teflon setup, a second line was added to actively introduce high-purity N<sub>2</sub> into the solution in the form of bubbles. This increased gas-liquid contact and facilitated the stripping of dissolved volatile species, which were then transported to the instrument for analysis.

By comparing the results from these three gas delivery approaches, we were able to obtain an approximate estimation of the volatile emissions—or *evolution*—associated with the HOCl solution under different sampling conditions.

The second approach, referred to as the nebulization experiment, was designed to simulate the introduction of HOCl solution in the form of droplets into a sealed, fixed-volume Teflon bag filled with either nitrogen or zero air—representing an idealized environment. By analyzing the composition of the gas within the bag after mixing with HOCl droplets, we aimed to investigate the chemical reactions and phenomena that may occur under specific environmental conditions.

For the *bag experiment*, three distinct testing methods were employed to assess the behavior and potential risks associated with nebulized HOCl mist in a controlled, enclosed environment:

**Dry House Air with Single Mist Introduction:** A Teflon bag was filled with dry house air, followed by the introduction of nebulized HOCl mist for five minutes. After allowing sufficient time for the mist to mix with the air inside the bag, the gas-phase composition was analyzed.

**Humidified House Air with Single Mist Introduction:** In this setup, house air was first humidified by passing it through a water-filled container before filling the Teflon bag. The same five-minute nebulization of HOCl mist and subsequent mixing and analysis were then conducted as in previous method.

**Dry House Air with Stepwise Mist Accumulation:** The Teflon bag was initially filled with dry house air. Nebulized HOCl mist was then introduced incrementally in small amounts. After each addition, the bag's contents were analyzed. This cycle was repeated until the measured signal approached the instrument's limit of quantification (LOQ).

Through these three testing strategies, we aimed to estimate the amount of nebulized HOCl mist that could lead to potentially hazardous concentrations in a non-ventilated, fixed-volume environment. Additionally, these experiments allowed us to assess the impact of humidity on the behavior and stability of HOCl in the gas phase.

The outcomes of this research are anticipated to provide insights into airborne chemical composition following use of HOCl disinfectants and to inform the development of regulatory measures.

### **3. Instrument**

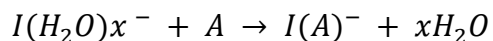
All analyses and data presented in this study were obtained using the High-Resolution Time-of-Flight Chemical Ionization Mass Spectrometer (HR-ToF-CIMS) housed at the University of Washington. This instrument, developed and operated by the Thornton Group, integrates a ToFwerk L-ToF mass spectrometer with a custom-built ionization and inlet system designed and validated in-house.

The HR-ToF-CIMS employs chemical ionization as its ionization technique, offering several advantages including high sensitivity, excellent chemical selectivity, and fine temporal resolution. The instrument achieves mass accuracy better than 10 ppm and provides a mass resolving power of at least 5000  $m/\Delta m$  (FWHM).

Chemical ionization is a soft ionization technique used in mass spectrometry, in which analyte molecules are ionized through chemical reactions with ions produced from reagent gas. This method significantly reduces molecular fragmentation, making it particularly advantageous for determining molecular weights and facilitating molecular identification. In this study,

iodomethane (CH<sub>3</sub>I) was employed as the reagent gas, with toluene added to absorb ultraviolet (UV) radiation in order to suppress UV interference on sample.

In this research, iodide (I<sup>-</sup>) was produced from CH<sub>3</sub>I as the reagent ion for chemical ionization. Iodide ions possess high electronegativity and exhibit a pronounced negative mass defect. These characteristics confer exceptional stability, making iodide less likely to form clusters with contaminant ions. As a result, iodide offers enhanced selectivity and lower detection limits when used as a reagent ion, making it the preferred choice for chemical ionization in this study. Iodide ions are generated through a high-voltage discharge and directed into a custom ion–molecule reaction (IMR) region, where they interact with analyte molecules in the gas phase. This process primarily results in the formation of iodide–analyte cluster ions via ion–molecule adduct formation.



The iodide-adduct ionization pathway is known for its minimal fragmentation, allowing the parent molecule's composition of the analyte to be largely preserved during ionization (Lee et al., 2014).

The formed iodide–analyte clusters pass through a low-pressure region within the instrument before entering the Time-of-Flight (TOF) analyzer. According to the operating principles of TOF mass spectrometry, all ions are imparted with the same kinetic energy by an applied electric field, enabling them to traverse the U-shaped flight tube. Because an ion's mass is inverse proportional to its flight time, ions can be distinguished and specified based on the time they reach the detector. A greater number of ions at a given mass results in a higher peak intensity, or

total ion counts (TICs), in the mass spectrum. In our setup, one mass spectrum is collected every second, allowing for real-time observation and analysis of the temporal evolution of the analytes' chemical composition.

## **Methodology**

(Photos of apparatus pictures shown in Appendix)

### **1. Solution Headspace Composition (Headspace experiment)**

#### **1.1. Apparatus**

For the headspace experiments, three distinct sampling configurations were implemented to characterize the gas-phase emissions of HOCl under varying conditions:

**Open-Air Diffusion Sampling:** The container holding the HOCl sample was placed near the inlet of the ion–molecule reaction (IMR) region, allowing the naturally volatilized headspace gases to mix with ambient room air. These mixed gases were then sampled into the CIMS instrument via its inlet flow for analysis. This setup represents the most direct and least controlled form of headspace sampling.

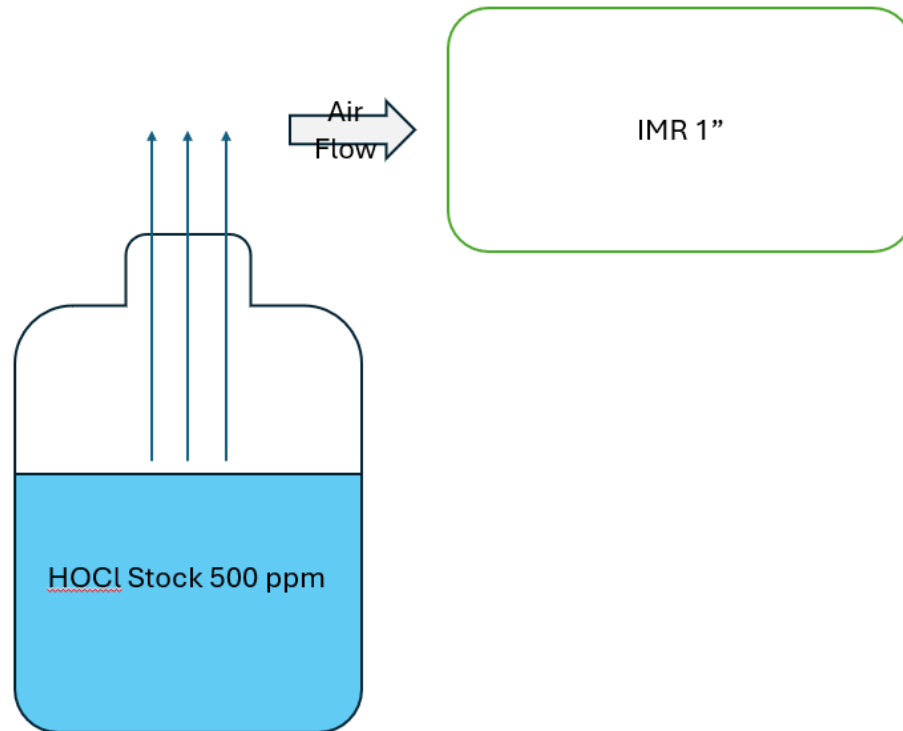


**Figure 1.** Direct HOCl headspace sampling. The bottle was composed of 3ml (10\*75mm) glass vials or the 2L amber bottle received from the manufacturer

**Sealed Inert Flow Sampling:** To isolate the headspace emissions from ambient air, a closed apparatus was constructed using Teflon tubing and ultra-high purity (UHP, >99.999%) nitrogen gas as the carrier. The system employed two 1/4" Teflon tubes connected to either end of a 1/2" Teflon tee via 1/4" to 1/2" adaptors. One of the 1/4" tubes delivered UHP N<sub>2</sub> into the system, while the other extended toward the 1" IMR inlet, carefully positioned to avoid contact with the inlet walls. The third port of the tee was fitted with a glass vial tube containing the HOCl sample. In this design, headspace gases evolved from the HOCl solution under inert conditions and were carried by the nitrogen stream directly to the IMR.

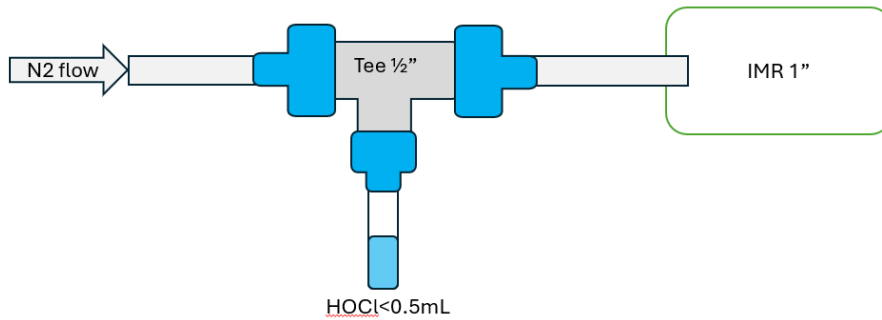


**Figure 2.** Sealed HOCl headspace gas delivery system. The N<sub>2</sub> flow could be altered from 0.005 LPM to 4 LPM. Lower flow would have no signal change, and higher flow would mess up the signal.

**Inert Flow with Bubbling Enhancement:** Building on the sealed system described above, a 1/8" hollow Teflon tube was inserted through the nitrogen delivery line and into the tee, with its outlet submerged below the surface of the HOCl solution. This enabled bubbling of nitrogen gas directly through the liquid sample, increasing gas–liquid contact and promoting more rapid and complete volatilization of headspace components. The resulting enriched headspace gas was then delivered to the IMR for analysis via the same tee outlet configuration.

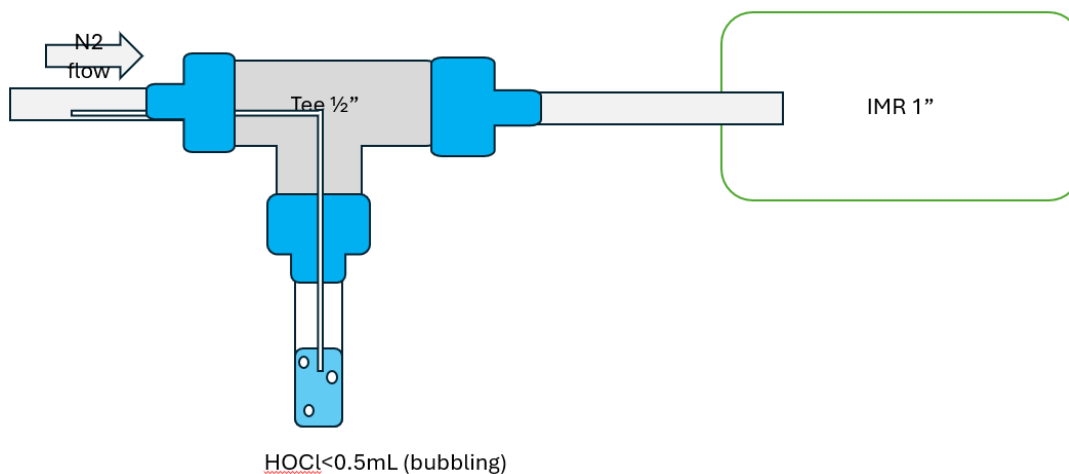


**Figure 3.** Sealed HOCl headspace gas delivery system with bubbling feature. The N<sub>2</sub> flow could be altered from 0.005 LPM to 4 LPM. Lower flow would have no signal change, and higher flow would mess up the signal.

These configurations allowed for a comparative evaluation of headspace evolution under ambient and controlled conditions, including both passive volatilization and active bubbling, thereby offering insights into the behavior of HOCl and its volatile byproducts under various sampling scenarios.

## 1.2. Experimental Procedure

Under standard conditions, the HOCl stock solution used in our experiments has a concentration of 500 ppm by mass. The ion–molecule reaction (IMR) tube of the chemical ionization mass spectrometer (CIMS) is directly connected to a mechanical pump responsible for removing waste gases. By adjusting the pump’s valve, the initial flow rate within the IMR is set to 10 liters per minute (LPM). Subsequently, 1.5 LPM of ultra-high-purity (UHP) nitrogen and 0.002 standard cubic centimeters per minute (sccm) of toluene are introduced into the system via flow rate controllers, reducing the IMR flow rate to approximately 8.5–8.7 LPM. This adjusted range represents the operational flow rate used throughout the experiments.

For the headspace experiments—excluding the direct headspace measurement—we typically place approximately 0.6 mL of the HOCl solution into a glass vial. We then introduce ultra-high purity nitrogen (UHP N<sub>2</sub>) at an initial flow rate of 0.005 LPM to carry the volatilized headspace gases into the IMR for analysis. This low N<sub>2</sub> flow rate facilitates the gentle transport of headspace constituents without significantly disturbing the equilibrium between the liquid and gas phases.

Depending on specific experimental requirements, we adjust the N<sub>2</sub> flow rate with a flow rate controller in the range of 0.005 LPM and 4 LPM—either increasing or decreasing it—to observe its effect on the detection signals of Cl<sub>2</sub> and HOCl.

## 2. Composition Upon Nebulization

### 2.1. Apparatus

To measure the trace gas composition resulting from the nebulization of the Briotech HOCl solution, we employed an apparatus consisting of a Teflon bag and a T-shaped gas-delivery system. The experimental setup is illustrated in Figure 4. The Teflon bag, with an approximate capacity of 640 liters, was equipped with two ¼” Teflon ports for gas inlet and outlet. This gas-delivery configuration was similar to that used in the headspace experiments, except the glass vial was replaced with the outlet flow from the bag. By adjusting the nitrogen flow rate, the bag’s output flow could be regulated, given the instrument’s constant intake through the ion–molecule reaction (IMR) region. For the experiments described, the nitrogen flow was set to 7.9 LPM, resulting in a bag output flow rate of 1.5 LPM.

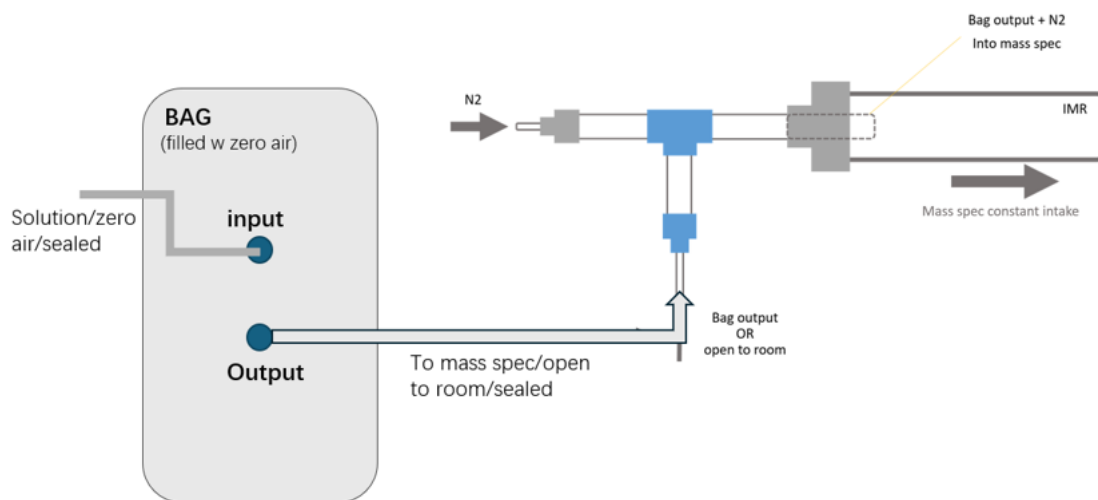


**Figure 4.** Bag air sampling set up including a Teflon bag (640 L) with two ¼” diameter holes for input/output flow and a Teflon tee set up similar to the headspace sampling set up shown in **Figure 2 and 3**. The original glass vial was replaced by a ½” tube and connected with the Teflon bag. The output flow rate from the Teflon bag can be adjusted by the variable UHP nitrogen flow.

The HOCl solution was nebulized using a Symdral Ultrasonic Cool Mist Humidifier, producing airborne droplets of the solution. This mist was transported into the bag via a combination of Tygon and Teflon tubing. To minimize mist loss during transfer, the outlet of the humidifier was sealed with parafilm and Kapton tape, including the interface between the humidifier tank and its control panel.

## **2.2. Experimental Procedure**

Prior to nebulization, the Teflon bag was flushed and filled with dry house air (for humidified nebulization experiment, the bag was filled with humidified house air). For each experiment, 125 mL of the 500 ppm HOCl solution is added to the humidifier tank. The volume of solution nebulized is estimated by measuring the remaining liquid in the tank after nebulization. For single-mist-introducing experiments, typically, the humidifier operates for 5 minutes on the 'max' setting, delivering mist into the bag's inlet port while the outlet remains sealed. Following nebulization, both ports are sealed for approximately 5–10 minutes to allow for gas mixing. The bag outlet is then connected to the instrument's gas-delivery system for 2–3 minutes to perform sampling. Afterward, the outlet is re-sealed while the instrument samples ambient room air for 10–20 minutes. This sampling cycle is repeated over 4 times to monitor the stability and magnitude of detected gas-phase signals.

For the stepwise mist accumulation experiments, all settings remained consistent with the standard protocol, except that the humidifier was operated multiple times rather than a single continuous run. In each step, the humidifier nebulized the HOCl solution for 0.5 to 1 minute, and this process was repeated until the reagent (Iodide) signal were titrated.

At the conclusion of bag sampling, the gas-delivery system is disconnected, and the output of a chlorine ( $\text{Cl}_2$ ) permeation device is introduced to the instrument. This enables direct instrument calibration and quantification of chlorine gas concentrations, reported in parts per trillion (ppt), both within the instrument and inside the Teflon bag.

## Results & Discussion

### 1. General Discovery

One important consideration in these experiments is that, unless the IMR is obstructed, the total ion counts (TICs) typically remain relatively stable.



**Figure 5.** Plot example for the obstructed IMR from nebulization experiments. (14:04~14:06) Full tee gas delivery system attached to the IMR with  $\text{N}_2$  flow sent. (14:06~14:17) Nothing attached to the IMR. (14:17~14:22) only the 1" to 1/2" reducer attached to the IMR. (14:22~14:23) Tee gas delivery system attached to the IMR without  $\text{N}_2$  flow sent. (after 14:23) Full tee gas delivery system attached to the IMR with  $\text{N}_2$  flow sent.

When the analyte concentration increases, an increase in sample ion signals can lead to a corresponding decrease in total reagent ion counts (TRICs). In this research, the TRICs equal to the sum of total ion counts of both  $\text{I}^-$  and  $\text{IH}_2\text{O}^-$ . A significant drop in TRICs indicates that the reagent ions have been titrated—i.e., consumed by reactions with excessive analyte molecules—

limiting further ion–molecule interactions. To ensure accurate quantification, analyte signals are normalized to TRICs, as this approach accounts for overall instrument signal stability and provides a more accurate representation of the sampled air.

$$\text{Normalized analyte signal} \left( \frac{\text{counts} * 1e6}{\text{TRICs}} \right)$$

$$= \text{raw analyte signal (counts)} * 1e6 / (\text{raw } I^- \text{ signal} + \text{raw } IH_2O^- \text{ signal})$$

However, once the TRICs become over-titrated, the normalized sample signals lose their reliability and can no longer be considered quantitatively valid.



**Figure 6.** Example for titration. Analytes entering the CIMS would cause the rapid drop of both  $I^-$  and  $IH_2O^-$  (reagent) and rise of analytes. If the reagent signals dropped too seriously, it means the reagents are titrated.

## 2. Headspace Experiments Results

In the absence of any gas delivery system, 0.6 mL of HOCl solution was placed in a glass vial positioned just outside the IMR inlet. Under these conditions, the headspace gases passively diffused in a static state, mixing with ambient room air before being drawn into the instrument for analysis. **Figure 7** presents the time series of normalized analyte signals obtained during this

experiment. The data show that, once equilibrium was reached and no external gas flow was introduced, only  $\text{Cl}_2$  exhibited a visible change in signal intensity, while HOCl and chloramines remained largely undetected, suggesting that their concentrations in the headspace were negligible or below the detection limit.

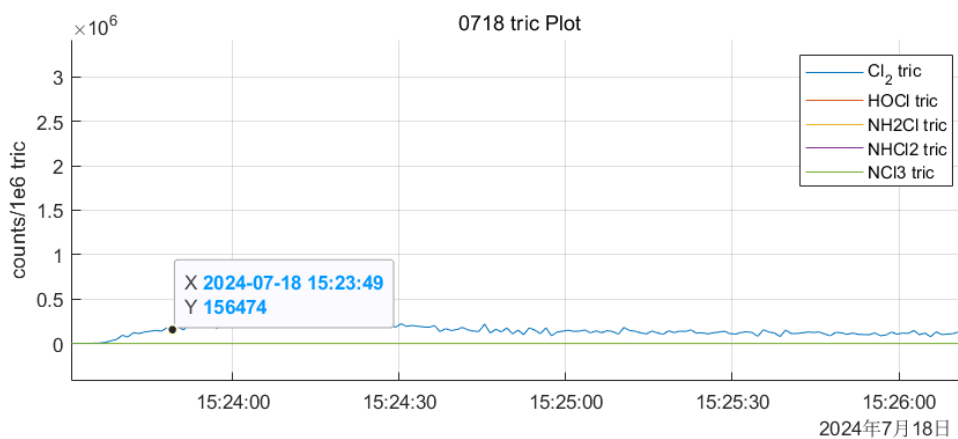


**Figure 7.** Time series of normalized  $\text{Cl}_2$ , HOCl, chloramine counts for direct headspace testing. Only  $\text{Cl}_2$  visible.

When the Teflon tee gas delivery system was introduced, the nitrogen ( $\text{N}_2$ ) flow actively perturbed the headspace gases, resulting in a dynamic sampling environment distinct from static headspace conditions. One key observation was that incorporating a bubbler led to a greater detectable signal for HOCl, compared to setups without bubbling. This enhancement prompted the frequent use of a bubbler in subsequent experiments to improve HOCl detection. As in previous trials, 0.6 mL of HOCl solution was used. The time series of normalized analyte signals from the headspace under different conditions is shown in Figures 8 and 9.

In **Figure 8**, the  $\text{N}_2$  delivery flow rate was initially set to 0.005 LPM (liters per minute). Under this low-flow condition,  $\text{Cl}_2$  dominated the detected signal, while HOCl and other analytes remained undetectable. At 14:23, the flow rate increased to 0.02 LPM. Following this

adjustment, a sharp increase in  $\text{Cl}_2$  signal was observed, likely due to enhanced transport of volatile compounds. Over time, as the system approached a new equilibrium, the  $\text{Cl}_2$  signal decreased and an  $\text{HOCl}$  signal began to emerge.

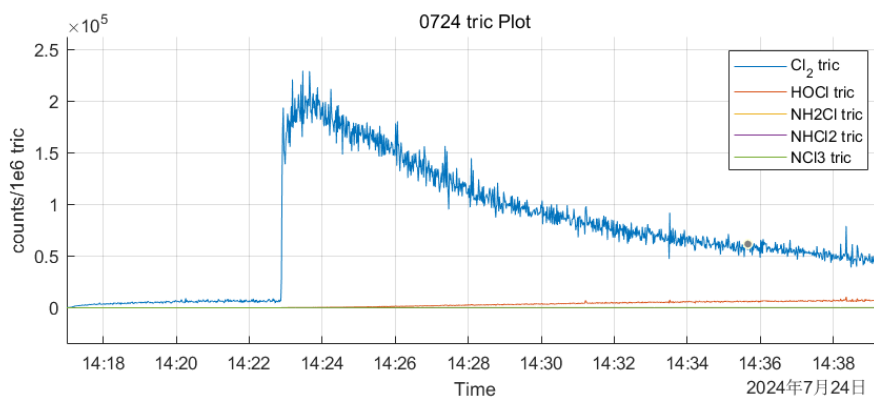


**Figure 8.** Time series of normalized  $\text{Cl}_2$ ,  $\text{HOCl}$ , chloramine counts for sealed headspace testing. From the beginning to 14:23 represents the evolution of volatile chlorine compounds under  $\text{N}_2$  flow rate of 0.005 LPM. From 14:23 to the end represents the evolution of volatile chlorine compounds under  $\text{N}_2$  flow rate of 0.02 LPM.

Given the observation that increasing the  $\text{N}_2$  flow rate enhanced the  $\text{HOCl}$  signal, we further investigated the effect of significantly increasing the flow rate on signal response. As shown in **Figure 9**, the  $\text{N}_2$  flow rate was first increased to 0.5 LPM. As expected, under this condition, the  $\text{HOCl}$  signal became dominant, while the  $\text{Cl}_2$  signal dropped to near-baseline levels.

Subsequently, the flow rate increased to 1 LPM, 2 LPM, 3 LPM, and finally 4 LPM. The  $\text{HOCl}$  signal continued to increase with flow rate to approximately 3 LPM. After 3 LPM, the  $\text{HOCl}$  stop increasing along with the flow rate.

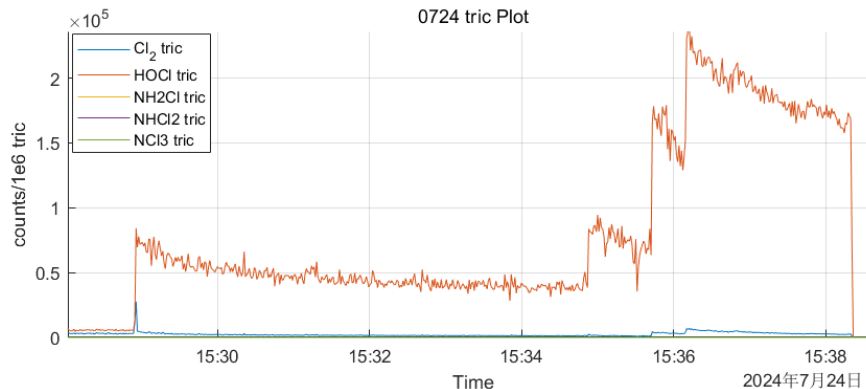


**Figure 9.** Time series of normalized  $\text{Cl}_2$ , HOCl, chloramine counts for sealed headspace testing. Each step here means an  $\text{N}_2$  flow rate increase. The first step was at 0.5 LPM, second step was at 1 LPM, third step was at 2 LPM, and the fourth step was at 3 and 4 LPM.

These trends suggest that under static or low-flow conditions,  $\text{Cl}_2$  is the predominant volatile compound present in the headspace of HOCl solution, while very little HOCl is detected.

However, at higher flow rates, the opportunities for HOCl to undergo self-decomposition or react with other species are greatly reduced, resulting in a greater fraction of volatile HOCl reaching the detector. From this, we can infer that in situations where large volumes of liquid HOCl solution are left to evaporate under ambient conditions, more  $\text{Cl}_2$ —rather than HOCl—is likely to be released into the air.

The gradual decrease in both HOCl and  $\text{Cl}_2$  signals over time, as observed in the figures, reflects the ventilated nature of the system—whether through static or dynamic headspace sampling.

Both the IMR and the  $\text{N}_2$  delivery simulate a ventilation effect, leading to an initial rapid increase followed by a decline in signal without reaching a plateau (Stubbs et al., 2023).

Regarding chloramines (mono-, di-, or trichloramine), no detectable signal was observed under any  $\text{N}_2$  flow condition. This suggests that while chloramines may be present, their concentrations or signal strengths are likely below the detection threshold and indistinguishable from instrumental noise.

### 3. Nebulization Experiments Results

To investigate the behavior of HOCl solution after droplet formation by a humidifier in a confined space, a fixed volume of HOCl solution was added to the humidifier, which then nebulized the liquid into a Teflon bag filled with either dry or humidified house air through a combination of Teflon and Tygon tubing. The resulting gas-phase contents of the bag were subsequently analyzed using a gas delivery system connected to the instrument.

Each single-time HOCl introduction into the bag was limited to 5 minutes of nebulization under maximum power. This duration was chosen based on comparative analysis showing that 5 minutes is the maximum nebulization time in dry air conditions that leads to a significant—but still analytically acceptable—drop in total reagent ion counts (TRICs) while maintaining analyte signals below TRICs. Although this level of titration is not ideal, it is considered barely acceptable for parts-per-trillion (ppt) quantification.

Repeated measurements confirmed that operating the humidifier at maximum power for 5 minutes typically consumes approximately 9 mL of solution.

In this set of nebulization experiments, we first examined the gas-phase composition inside the Teflon bag following a single 5-minute nebulization of HOCl solution into dry house air. **Figure 10** presents the time series of normalized signals for selected analytes of interest. As shown, Cl<sub>2</sub> is the dominant species detected in the bag, with HOCl also clearly present. Trichloramine was observed as well, whereas monochloramine and dichloramine were not detected. Furthermore, the levels of all analytes remained relatively stable over time, showing only a slight and gradual decrease.

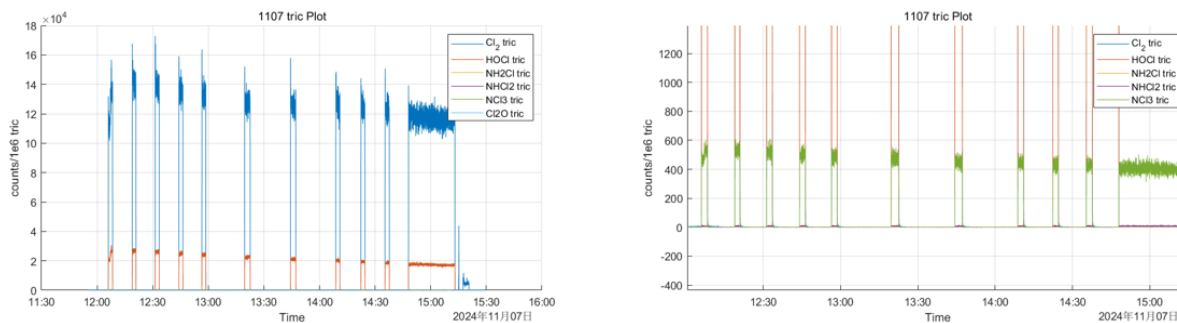


**Figure 10.** Timeseries for normalized analyte signals under 5-minute HOCl solution nebulization in the bag with dry house air. (Left) Full plots. (Right) Zoom-in plots to enhance visibility of the chloramines signals.

Calibration was conducted by introducing chlorine gas from a Cl<sub>2</sub> permeation tube into the IMR for a fixed period following each experiment. The Cl<sub>2</sub> permeation tube was maintained at approximately 40 °C to ensure a stable and known emission rate of Cl<sub>2</sub> gas. The mass of the permeation tube was recorded before and after calibration to determine the total mass of Cl<sub>2</sub> released during the calibration interval, allowing calculation of the effective emission rate (in ng/min).

Using this emission rate, along with the atomic mass of chlorine (70.9 g/mol) and the flow rate correction through IMR flow rate, the expected concentration of Cl<sub>2</sub> introduced into the system (in ppt) during calibration was calculated. The average normalized Cl<sub>2</sub> signal observed during calibration was then divided by the expected Cl<sub>2</sub> concentration to determine the instrument sensitivity to Cl<sub>2</sub>, expressed as (10<sup>6</sup>counts/TRICs)/ppt.

$$\begin{aligned}
 & \text{Sensitivity} \left( \frac{\frac{\text{counts} * 1e6}{\text{TRICs}}}{\text{ppt}} \right) \\
 &= \frac{\text{Normalized calibration analyte signal} \left( \frac{\text{counts} * 1e6}{\text{TRICs}} \right)}{\text{Expected calibration analyte concentration (ppt)}}
 \end{aligned}$$

The Cl<sub>2</sub> concentration during experiments was subsequently quantified by dividing the normalized Cl<sub>2</sub> signal by this sensitivity, yielding the concentration in ppt.

$$\text{Analyte Concentration (ppt)} = \frac{\text{Normalized analyte signal} \left( \frac{\text{counts} * 1e6}{TRICs} \right)}{\text{sensitivity} \left( \frac{\text{counts} * 1e6}{\text{ppt}} \right)}$$

**Figure 11** presents the time-resolved concentration profile of Cl<sub>2</sub> observed during the experiment. Approximately, the measured Cl<sub>2</sub> concentration here was 1.26e5 ppt, 0.126 ppm of Cl<sub>2</sub> in IMR.

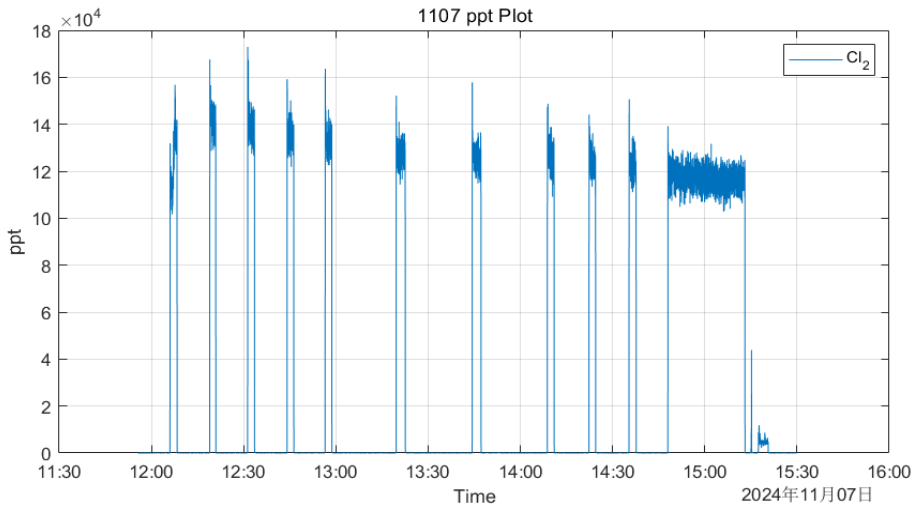


**Figure 11.** Timeseries for Cl<sub>2</sub> concentration in ppt. This was calculated by using normalized counts / sensitivity.

By flowrate correction:

$$C_{bag} = C_{IMR} \cdot \frac{F_{IMR}}{F_{bag}}$$

0.126 ppm of Cl<sub>2</sub> in IMR means 0.73 ppm of Cl<sub>2</sub> in bag.

Next, we estimate the expected HOCl concentration in the bag. A total of 9 mL of HOCl solution was consumed during nebulization, and we assume that the entire volume was introduced into the Teflon bag. The solution had a concentration of 500 ppm by mass (i.e., 500 mg of HOCl per kg of water). Assuming the density of water is 1 g/mL, the total mass of HOCl introduced is approximately 4.5 mg. Using the molar mass of HOCl (52.46 g/mol), the molar concentration of air at standard temperature and pressure (0.0446 mol/L), and the volume of the bag (640 L), we estimate that the expected HOCl concentration in the bag is approximately 3 ppmv.

$$\frac{\text{mol of solute}}{\text{volume of solvent}} = \text{concentration of solution}$$

$$\frac{4.5 \text{ mg} * \frac{1 \text{ g}}{1000 \text{ mg}}}{52.46 \frac{\text{g}}{\text{mol}}} = 1.3e - 7 \frac{\text{mol}}{\text{L}}$$

$$\frac{1.3e - 7 \frac{\text{mol}}{\text{L}}}{0.0446 \frac{\text{mol}}{\text{L}} * \frac{1}{1000} \frac{\text{L}}{\text{mL}}} = 0.003 \frac{\text{mL}}{\text{L}} = 3 \text{ ppmv}$$

Since the HOCl solution is the sole source of chlorine atoms introduced into the Teflon bag, the theoretical maximum chlorine atom concentration is 3 ppm, assuming complete volatilization and no chemical loss. According to the measurements and calculations shown in Figure 11, approximately 0.73 ppm of Cl<sub>2</sub> was detected in the bag, corresponding to 1.46 ppm of chlorine atoms.

Furthermore, as reported in the literature, the relationship between an analyte's binding enthalpy with iodide and its ionization sensitivity can be described by the following empirical equation:

$$S_i \propto \Delta H_i$$

$$\frac{S_i}{S_{ref}} = \frac{\Delta H_i}{\Delta H_{ref}}$$

(Robinson et al., 2022) (Lopez-Hilfiker et al., 2016)

$S_i$  is the sensitivity of the unknown compound,  $S_{ref}$  is the sensitivity of the known compound;  $\Delta H_i$  is the binding enthalpy of the unknown compound, and  $\Delta H_{ref}$  is the binding enthalpy of the known compound. Because the binding enthalpies of HOCl and Cl<sub>2</sub> with iodide are very similar (Binding enthalpy of HOCl = 17.5, Binding enthalpy of Cl<sub>2</sub> = 17.4), their sensitivities in iodide-based chemical ionization mass spectrometry are expected to be nearly equivalent. Based on this assumption, and considering the signal ratio shown in Figure 10, the concentration of HOCl in the bag is estimated to be approximately one-fifth that of Cl<sub>2</sub>, or about 0.146 ppm. This corresponds to an additional 0.146 ppm of chlorine atoms in the form of HOCl. Assuming no further decomposition of HOCl into other chlorine-containing species, the total post-experiment chlorine atom concentration in the bag would be approximately 1.606 ppm.

This value is significantly lower than the theoretical input of 3 ppm chlorine atoms, indicating a difference of about 46%. However, this deviation is reasonable considering the number of assumptions made throughout the estimation. For instance, the nebulized volume (9 mL) was determined by the difference between the volumes of HOCl solution added to and retrieved from

the humidifier, which may include losses due to spillage, residual liquid, or measurement uncertainty. Additionally, mist leakage from the humidifier unit and the presence of other volatile chlorine species not accounted for in this analysis (besides  $\text{Cl}_2$ ,  $\text{HOCl}$ , and  $\text{NCl}_3$ ) could also contribute to the observed loss. Therefore, the 46% difference between expected and measured chlorine content is understandable within the experimental limitations.

After evaluating the behavior of  $\text{HOCl}$  droplets in dry house air, we introduced humidity into the system by passing the house air through a bubbler filled with water, increasing the relative humidity (RH) from approximately 5% to 60%. All other experimental conditions remained unchanged, including the single 5-minute  $\text{HOCl}$  nebulization. **Figure 12** shows the time series of raw (unnormalized) signals for  $\text{I}^-$ ,  $\text{IH}_2\text{O}^-$ ,  $\text{ICl}_2^-$ ,  $\text{IHOCl}^-$ , and  $\text{INCl}_3^-$ . As before, no signals for monochloramine or dichloramine were observed.

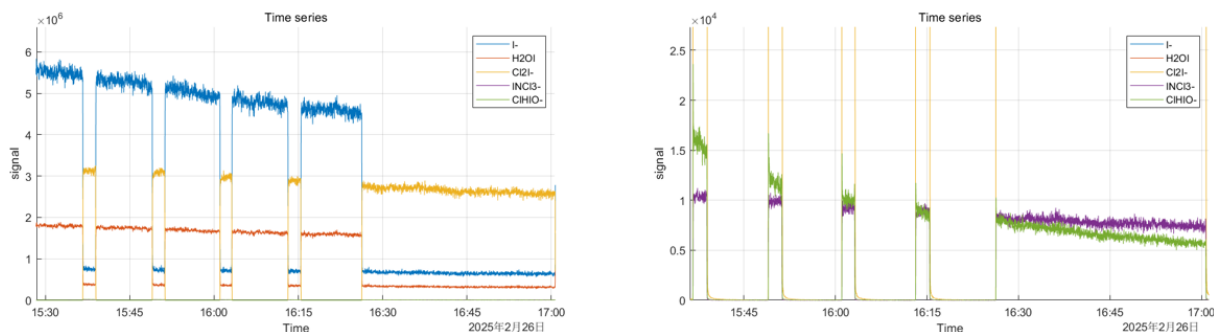
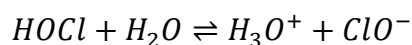


**Figure 12.** Timeseries for raw analyte signals under 5-minute  $\text{HOCl}$  solution nebulization in the bag with humid house air. (Left) Full plots. (Right) Zoom-in plots to enhance chloramines and  $\text{HOCl}$ .

Normalization was not possible for this dataset because the  $\text{Cl}_2$  signal was excessively high and effectively suppressed the reagent ion signals. Attempting to normalize under these conditions would yield artificially inflated values for the analytes, rendering quantification unreliable. Nonetheless, valuable qualitative insights can still be drawn from the raw signal trends.

Under high humidity, a greater fraction of HOCl appeared to decompose into Cl<sub>2</sub>, and the signal intensity of HOCl was comparable to that of NCl<sub>3</sub>. Interestingly, after the initial stabilization of the headspace composition, both Cl<sub>2</sub> and NCl<sub>3</sub> signals remained relatively constant, whereas the HOCl signal exhibited a clear declining trend. This suggests that under elevated humidity, HOCl undergoes either enhanced self-decomposition due to its rate-constant increases with RH, or its reactions with water vapor, leading to its depletion over time.



To identify an optimal nebulization duration beyond the standard 5-minute protocol—one that minimizes excessive titration of reagent ion signals—and to investigate the possibility of a maximum nebulization time after which Cl<sub>2</sub> concentration in the bag reaches equilibrium, we conducted stepwise nebulization experiments under dry house air conditions. HOCl solution was incrementally nebulized into the Teflon bag in multiple steps, with a total cumulative nebulization time of 20 minutes. Figure 13 presents a representative time series of the raw analyte signals obtained from this experiment.

As in **Figure 12**, **Figure 13** also displays raw (unnormalized) signals due to strong analyte concentrations that suppressed reagent ion signals. Cl<sub>2</sub> remained the dominant chlorine-containing byproduct, followed by HOCl, while trichloramine was consistently observed but at lower signals. Monochloramine and dichloramine signals were not detected throughout the experiment.

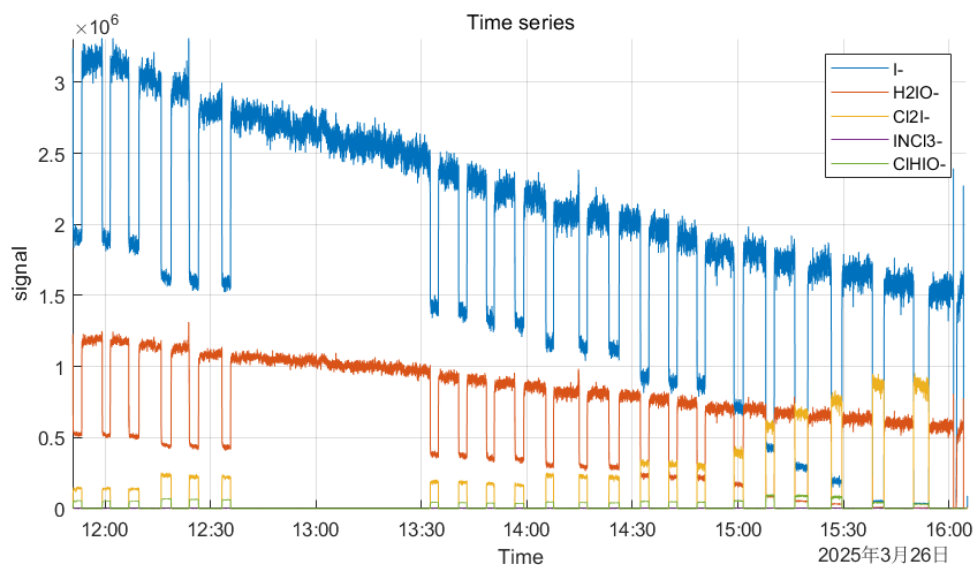


**Figure 13.** Timeseries for raw signals under stepwise (total 20 minutes) HOCl solution nebulization in the bag with dry house air. (11:50~12:10) 1<sup>st</sup> 1-minute nebulization, tested 3 times. (12:16~12:35) 2<sup>nd</sup> 1-minute nebulization, tested 3 times. (12:35~13:32) 3<sup>rd</sup> 1-minute nebulization, waited for 1 hour. (13:32~13:50) tested 3 times. (13:56~13:59) 4<sup>th</sup> 1-minute nebulization, line clogged so no mist addition into the bag at all. (14:05~14:26) real 4<sup>th</sup> 1-minute nebulization, tested 3 times. (14:32~14:50) 5<sup>th</sup> 1-minute nebulization, tested 3 times. (14:58~15:01) 1<sup>st</sup> 2-minute nebulization, tested 1 time. (15:07~15:10) 2<sup>nd</sup> 2-minute nebulization, tested 1 time. (15:16~15:20) 3<sup>rd</sup> 2-minute nebulization, tested 1 time. (15:26~15:29) 4<sup>th</sup> 2-minute nebulization, tested 1 time. (15:38~15:41) 5-minute nebulization, tested 1 time. (15:50~15:53) 2-minute nebulization, tested 1 time.

At a total nebulization time of 4 minutes (13:56–13:59), reagent ion signals appeared for the last time above those of the chlorine-containing analytes, after which severe titration occurred. The data suggest that even after 20 minutes of continuous nebulization, Cl<sub>2</sub> levels in the bag had not reached equilibrium. Moreover, reagent ion suppression was already substantial after just 1 minute of HOCl droplet introduction, indicating a very rapid response in the gas phase chemistry.

Interestingly, when HOCl droplets were introduced for only 1 minute and then the bag was left undisturbed for an hour (12:35–13:32), the levels of Cl-containing compounds remained nearly

identical to those measured directly after droplet introduction. This strongly suggests a leak in the bag, which allows for slow loss of Cl compounds over time.

Additionally, both **Figures 12 and 13** show a gradual decline in reagent ion signals over time. This decline is frequently observed when the tee gas delivery system remains connected to the IMR inlet for extended periods. We hypothesize that this may be due to partial obstruction of the IMR flow path, leading to a sustained decrease in  $I^-$  signal. Alternatively, the oxidation of iodide by residual HOCl may also contribute to this phenomenon.

Across all nebulization experiments, unless additional HOCl droplets were introduced, the levels of chlorine-containing species remained nearly constant, exhibiting only marginal decreases. This observation reinforces the notion that, in the absence of active ventilation,  $Cl_2$ ,  $NCl_3$ , and similar compounds persist in the headspace. This finding highlights a significant safety concern: the use of chlorine-based disinfectants in poorly ventilated or enclosed environments may lead to prolonged exposure to hazardous volatile chlorine species.

Based on the results above and the observed trends from the stepwise nebulization experiments, we can make further assumptions to project realistic scenarios. As shown in **Figure 13**, the levels of all analytes appear to increase roughly in proportion to the total nebulization time, with  $Cl_2$  and HOCl showing the most prominent responses. Building upon the stepwise nebulization experiments, we further reduced the nebulization interval to 10 seconds per nebulization to minimize the depletion of reagent ion signals and keep them within a quantifiable range.

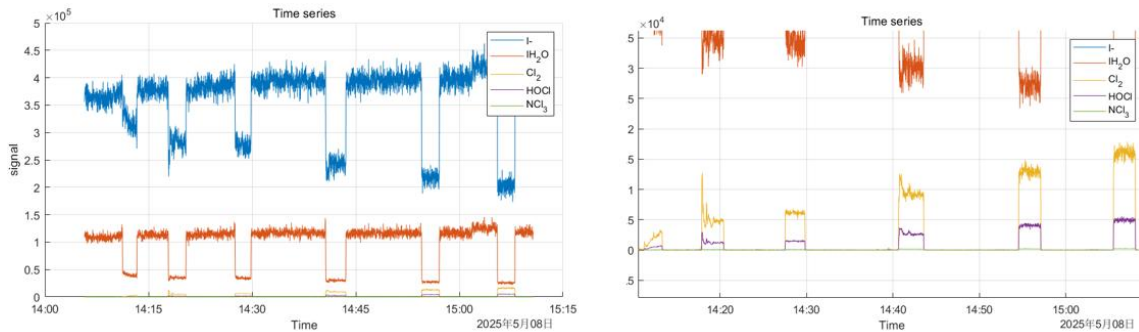


**Figure 14.** Timeseries of raw signals under stepwise (total 60 seconds) HOCl solution nebulization in the bag with dry house air. (Left) Full plots. (Right) Zoom-in plots to enhance chloramines and HOCl.

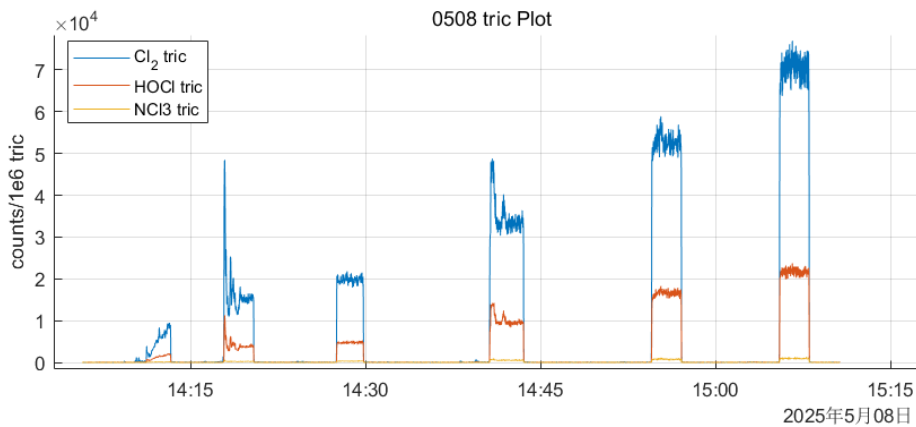
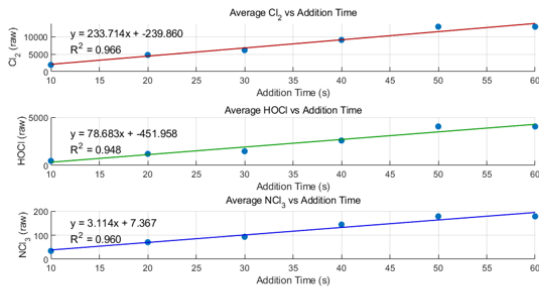
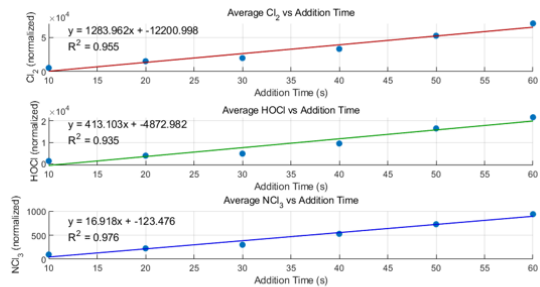


**Figure 15.** Timeseries of nebulized analyte signals under stepwise (total 60 seconds) HOCl solution nebulization in the bag with dry house air.

**Figure 14** and **Figure 15** present the time series of raw and normalized signals resulting from each 10-second nebulization interval. As shown in the figure, when the Teflon bag was loaded with HOCl mist for 10, 20, and 30 seconds, the reduction in reagent ion signals remained within an acceptable range for quantification. However, the subsequent three HOCl inputs caused excessive signal depletion, causing those points unsuitable for accurate quantification. Nevertheless, all six data points can still be used to establish the overall relationship between analyte concentrations and nebulization time.



Raw analyte signals vs addition time



Normalized analyte signals vs addition time

**Figure 16.** Scatter plots showing the average analyte signals as a function of the corresponding nebulization time. (Left) Raw analyte signals. (Right) Normalized analyte signals.

**Figure 16** are scatter plots generated from each average analyte signal in **Figures 14** and **15**, plotted against their corresponding nebulization times. The linear fit lines and associated R<sup>2</sup> values clearly indicate that, for both raw and normalized signals, the concentrations of all three analytes exhibit a strong linear correlation with nebulization time.

Based on this observed linear relationship and the fact that the first three data points fall within the quantifiable range, we isolated these points from the normalized Cl<sub>2</sub> signal scatter plot for further quantitative analysis.

Based on the same calculation procedure previously used to determine the “Analyte Concentration (ppt),” we calculated the Cl<sub>2</sub> concentration in the IMR corresponding to the first three data points. Then, applying the same flow rate correction method, we derived the Cl<sub>2</sub> concentrations within the Teflon bag.

Using the dilution formula:

$$C_{bag}V_{bag} = C_{room}V_{room}$$

and taking the bag volume  $V_{\text{bag}}=640$  L and the room volume  $V_{\text{room}}=27$  m<sup>3</sup>, we extrapolated the expected Cl<sub>2</sub> concentrations in a 27 m<sup>3</sup> room with no additional loss mechanism (e.g., surface adsorption or ventilation) following 10, 20, and 30 seconds of HOCl mist generated by the nebulizer. The resulting scatter plot, shown in **Figure 17**, illustrates how Cl<sub>2</sub> concentration increases proportionally with nebulization time under ideal mixing conditions.

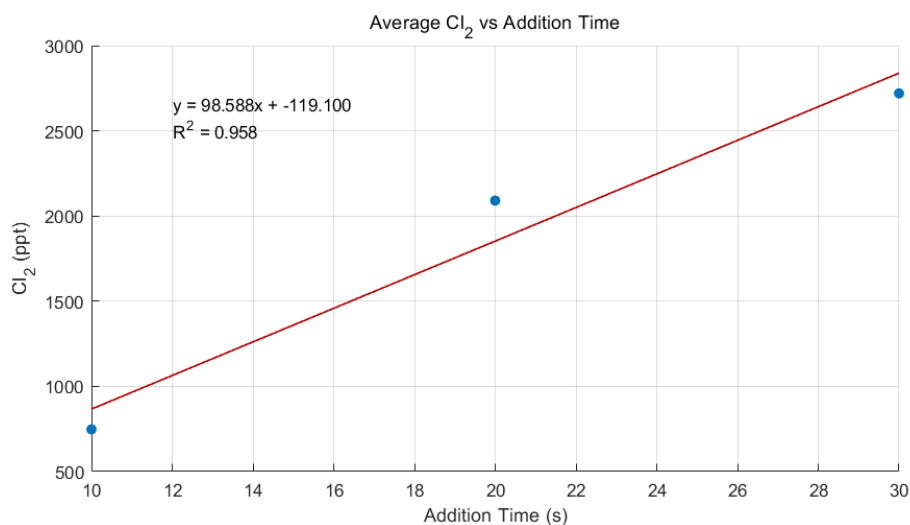


**Figure 17.** Scatter plots showing the Cl<sub>2</sub> concentration in a 27 m<sup>3</sup> room as a function of the corresponding nebulization time.

Based on the linear equation shown in **Figure 17**, under an ideal 27 m<sup>3</sup> room, it would require approximately 10144 seconds—or about 2.8 hours—of continuous HOCl mist nebulization to reach the hazardous 1 ppm Cl<sub>2</sub> threshold.

## Conclusions

This study investigated the volatilization behavior and gas-phase composition of commercial hypochlorous acid (HOCl) solutions under varying delivery and environmental conditions using a time-of-flight chemical ionization mass spectrometry (TOF-CIMS) setup. This HOCl solution combined with electrolyte water is a novel formulation, distinct from the common chlorine

bleach (NaOCl) cleaners found on the market. Unlike bleach, which is more alkaline, the HOCl solution has a more neutral pH, making it milder and potentially safer for various applications. Given that the TOF-CIMS produced clear and visualized time-resolved mass spectra, it demonstrates the instrument's capability to successfully identify and quantify gaseous chlorine-containing byproducts.

From headspace experiments, we demonstrate that at low nitrogen flow rates or at equilibrium state, Cl<sub>2</sub> dominates the volatile headspace species, while HOCl becomes increasingly detectable only when the delivery flow rate is substantially increased, minimizing its self-decomposition and conversion during transport.

Upon nebulization, HOCl solution is introduced into a closed environment, with Cl<sub>2</sub> consistently observed as the dominant gas-phase chlorine product, followed by HOCl and NCl<sub>3</sub>. Notably, no detectable signals for mono- or dichloramine were observed under any tested condition.

Stepwise nebulization experiments reveal that Cl<sub>2</sub> levels do not reach equilibrium under dry house air condition even after prolonged (20-minute) HOCl droplet introduction. The observed decline in reagent ion signals over time suggests potential obstruction at the IMR inlet, which may impair ion transmission efficiency and affect analyte detection sensitivity. The minimal changes in chlorine compound levels during long pausing period indicates probable leakage from the experimental bag setup.

Importantly, high humidity conditions were found to accelerate HOCl decomposition and enhance Cl<sub>2</sub> formation, altering the partitioning and persistence of volatile chlorine species.

These findings collectively underscore the complexity of HOCl-based disinfectant volatilization

dynamics, particularly in humid or poorly ventilated environments. The prolonged persistence of reactive chlorine gases such as  $\text{Cl}_2$  and  $\text{NCl}_3$  in enclosed spaces raises important considerations for indoor air quality and human exposure risks during the use of chlorine-containing cleaning products.

In future work, I plan to design a new type of headspace experiment in which a very small volume (on the order of microliters) of  $\text{HOCl}$  solution is applied directly onto the inner wall of the IMR inlet using a pipette. This approach is intended to reduce the headspace traveling time and minimize opportunities for  $\text{HOCl}$  to undergo further reactions, thereby serving as a complementary method to the static headspace experiments.

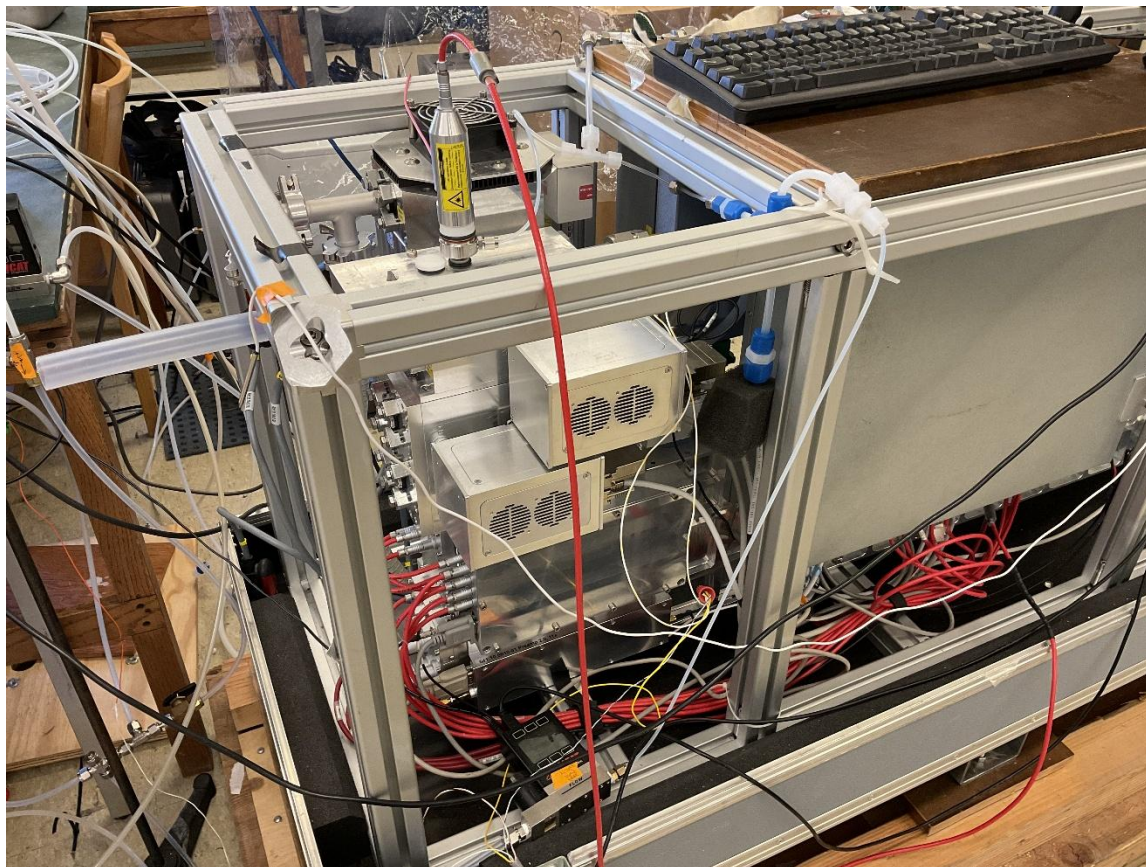
Additionally, while we have identified the safe  $\text{HOCl}$  nebulization duration under ideal conditions in a real indoor space, it is important to further consider other influencing factors that may affect  $\text{Cl}_2$  levels—such as the presence of a ventilation system and surface absorption effects. These factors could alter the actual accumulation and persistence of chlorine-containing byproducts, and thus should be incorporated into future risk assessments and experimental designs.

## Reference

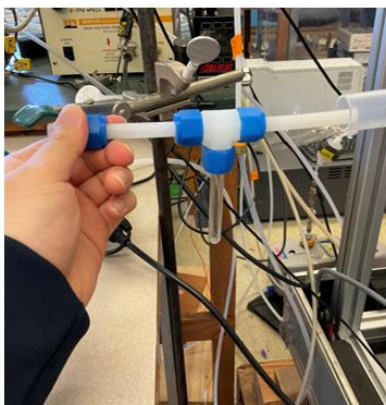
1. Winterbourn C.C. *Biological reactivity and biomarkers of the neutrophil oxidant, hypochlorous acid. Toxicology.* Volumes 181–182, 2002, Pages 223–227. ISSN 0300-483X. doi:10.1016/S0300-483X(02)00286-X.
2. Wong J.P.S., Carslaw N, Zhao R, Zhou S, Abbatt, J.P.D. *Observations and impacts of bleach washing on indoor chlorine chemistry. Indoor Air.* 2017; 27: 1082–1090. <https://doi.org/10.1111/ina.12402>
3. Stubbs A.D, Lao M, Wang C, Abbatt J. P. D, Hoffnagle J, VamdemNper T. C, Kahan, T. F. *Near-source hypochlorous acid emissions from indoor bleach cleaning. Environ. Sci.: Processes Impacts, 2023,25, 56-65.* <https://doi.org/10.1039/D2EM00405D>
4. William A. Rutala, David J. Weber, Healthcare Infection Control Practices Advisory Committee (HICPAC). *Disinfection And Sterilization Guideline (page 10 of 45). Infection Control.* November 28, 2023. <https://www.cdc.gov/infection-control/hcp/disinfection-sterilization/chemical-disinfectants.html#toc>
5. Boguski, TK. Understanding Units of Measurement. Environmental Science and Technology Briefs for Citizens, Issue 2. 2006.
6. Ha Y, Kim Y, Song E, Yoo HJ, Kwon J.H. *Development of a personal passive air sampler for estimating exposure to effective chlorine while using chlorine-based disinfectants. Indoor Air.* 2021 Mar;31(2):557-565. doi: [10.1111/ina.12747](https://doi.org/10.1111/ina.12747). Epub 2020 Oct 7. PMID: 32978992; PMCID: PMC7537288.
7. Mattila J.M, Lakey P.S.J, Shiraiwa M, Wang C, Abbatt J.P.D, Arata C, Goldstein A.H, Ampollini L, Katz E.F, DeCarlo P.F, Zhou S, Kahan T.F, Cardoso-Saldaña F.J, Ruiz L.H, Abeleira A, Boedicker E.K, Vance M.E, Farmer D.K. *Multiphase Chemistry Controls Inorganic Chlorinated and Nitrogenated Compounds in Indoor Air during Bleach Cleaning.* Environmental Science & Technology, Volume 54, Issue 3. 2020. doi: [10.1021/acs.est.9b05767](https://doi.org/10.1021/acs.est.9b05767)
8. Lindberg JE, Quinn MM, Gore RJ, Galligan CJ, Sama SR, Sheikh NN, Markkanen PK, Parker-Vega A, Karlsson ND, LeBouf RF, Virji MA. *Assessment of home care aides' respiratory exposure to total volatile organic compounds and chlorine during simulated bathroom cleaning: An experimental design with conventional and "green" products.* J Occup Environ Hyg. 2021 Jun;18(6):276-287. doi: [10.1080/15459624.2021.1910280](https://doi.org/10.1080/15459624.2021.1910280). Epub 2021 May 18. PMID: 34004120; PMCID: PMC8898565.
9. MASAYUKI ISHIHARA, KAORU MURAKAMI, KOICHI FUKUDA, SHINGO NAKAMURA, MASAHIRO KUWABARA, HIDEMI HATTORI, MASANORI FUJITA, TOMOHARU KIYOSAWA, HIDETAKA YOKOE, *Stability of Weakly Acidic Hypochlorous Acid Solution with Microbicidal Activity, Biocontrol Science, 2017, Volume 22, Issue 4, Pages 223-227, Released on J-STAGE December 26, 2017, Online ISSN 1884-0205, Print ISSN 1342-4815,* <https://doi.org/10.4265/bio.22.223>.
10. Lee, Ben H.; Lopez-Hilfiker, Felipe D.; Mohr, Claudia; Kurtén, Theo; Worsnop, Douglas R.; Thornton, Joel A. *An Iodide-Adduct High-Resolution Time-of-Flight Chemical-Ionization Mass Spectrometer: Application to Atmospheric Inorganic and Organic Compounds. Environmental Science & Technology.* 2014. doi: [10.1021/es500362a](https://doi.org/10.1021/es500362a)

11. Robinson, M. A., Neuman, J. A., Huey, L. G., Roberts, J. M., Brown, S. S., and Veres, P. R.: Temperature-dependent sensitivity of iodide chemical ionization mass spectrometers, *Atmos. Meas. Tech.*, 15, 4295–4305, <https://amt.copernicus.org/articles/15/4295/2022/>, 2022.
12. Lopez-Hilfiker, F. D., Iyer, S., Mohr, C., Lee, B. H., D'Ambro, E. L., Kurtén, T., and Thornton, J. A.: Constraining the sensitivity of iodide adduct chemical ionization mass spectrometry to multifunctional organic molecules using the collision limit and thermodynamic stability of iodide ion adducts, *Atmos. Meas. Tech.*, 9, 1505–1512, <https://amt.copernicus.org/articles/9/1505/2016/>, 2016.

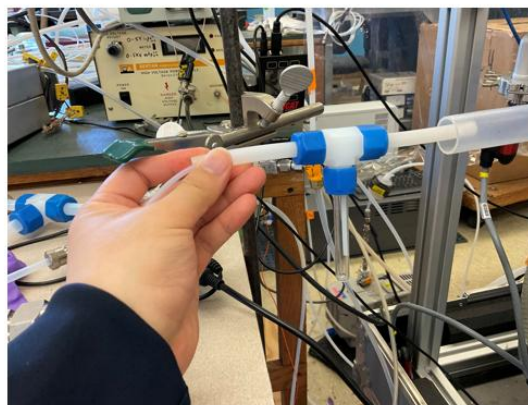
## Appendix



Appendix 1. Picture of ToF-CIMS. The metal box with one plastic tube is customized IMR. The object at the top of the IMR with a red wire connected is the vuv lamp for generating iodide ions. The rest is the spectrometer.



Tee gas delivery system  
(Without bubbler)



Tee gas delivery system  
(With bubbler)

7

Appendix 2. Pictures of headspace experiment apparatus. The left tube of the tee was supposed to connect with nitrogen gas. It was just a demonstration.



The bag itself



The tee gas delivery ststem

Appendix 3. Pictures of the bag and the gas delivery system for nebulization experiments. The bag in the picture is in its flat state (no gas/air added)

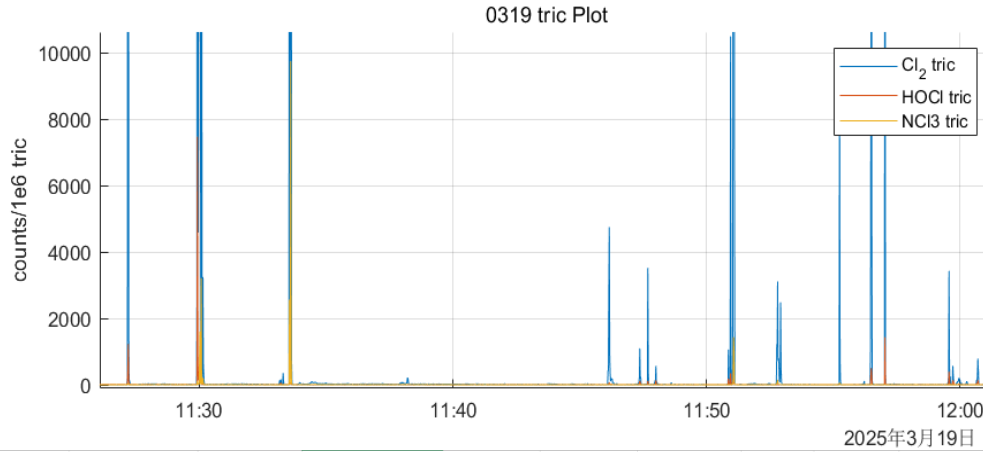


The nebulizer  
(Tape to seal the connection)



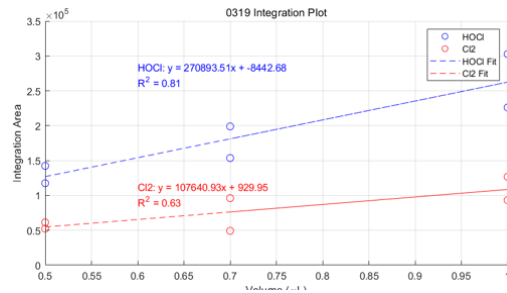
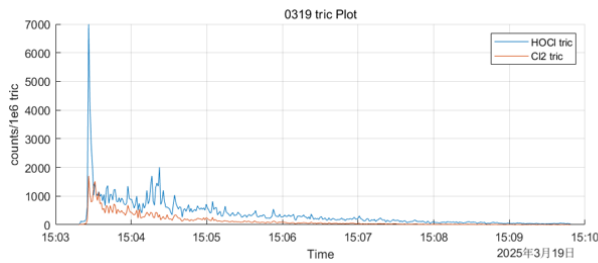
The seal of the nebulizer port  
(Non-circular port hole)

Appendix 4. (Left) The picture of the nebulizer we used for HOCl solution nebulization. Top is the tank for solution, bottom is the control panel, use tape to seal the connection to avoid leak. (Right) The picture of mist output port. The port hole is non-circular, so we sealed it with parafilm and tape to avoid leak.



wipe distance (cm)	solution volume (mL)	waiting time (s)	Cl2 highest counts/1e6 ppt						
25	1	10	52850.4						
25	1	10	609403	312502	180233				
25	1	10	383287	194122					
50	1	10	N/A						
50	1	10	N/A						
25	0.2	10	N/A						
25	0.2	10	N/A						
25	0.1	300	N/A (instant)	4751.09 (1 min)	1095 (2 min)	3522 (2 min)	567 (2 min)	1059 (wiping)	10502.5 (wiping)
25	0.1	10		3114	2486				
25	0.1	10		9786					
25	0.1	300	23180.1 (instant)	33614.9 (1 min)	3431.92 (3 min)	13518.5 (wiping)			

Appendix 5. (Top) Normalized signals for Cl<sub>2</sub>, HOCl, NCl<sub>3</sub> during a wipe testing using the HOCl solution. We just roughly wipe the HOCl solution on our lab table next to the IMR inlet. (Bottom) Data for the wiping test. The data here is too random to have formal conclusions.



Appendix 6. (Left) Cl<sub>2</sub> and HOCl example evolution while 0.7 μL of HOCl solution places in IMR inlet. (Right) relation between the integrated area of the range of analytes evolution and applied HOCl volume. The relation seems linear, but not representative.